

AD-A050 309

BALLISTIC RESEARCH LABS ABERDEEN PROVING GROUND MD
COHERENCE RETENTION DURING ROTATIONALLY INELASTIC COLLISIONS OF--ETC(U)
OCT 77 T A CAUGHEY, D R CROSLY

F/G 7/4

UNCLASSIFIED

BRL-2021

NL

| OF |
AD
A050309



BRL N 2021

BRL

9
AS
12

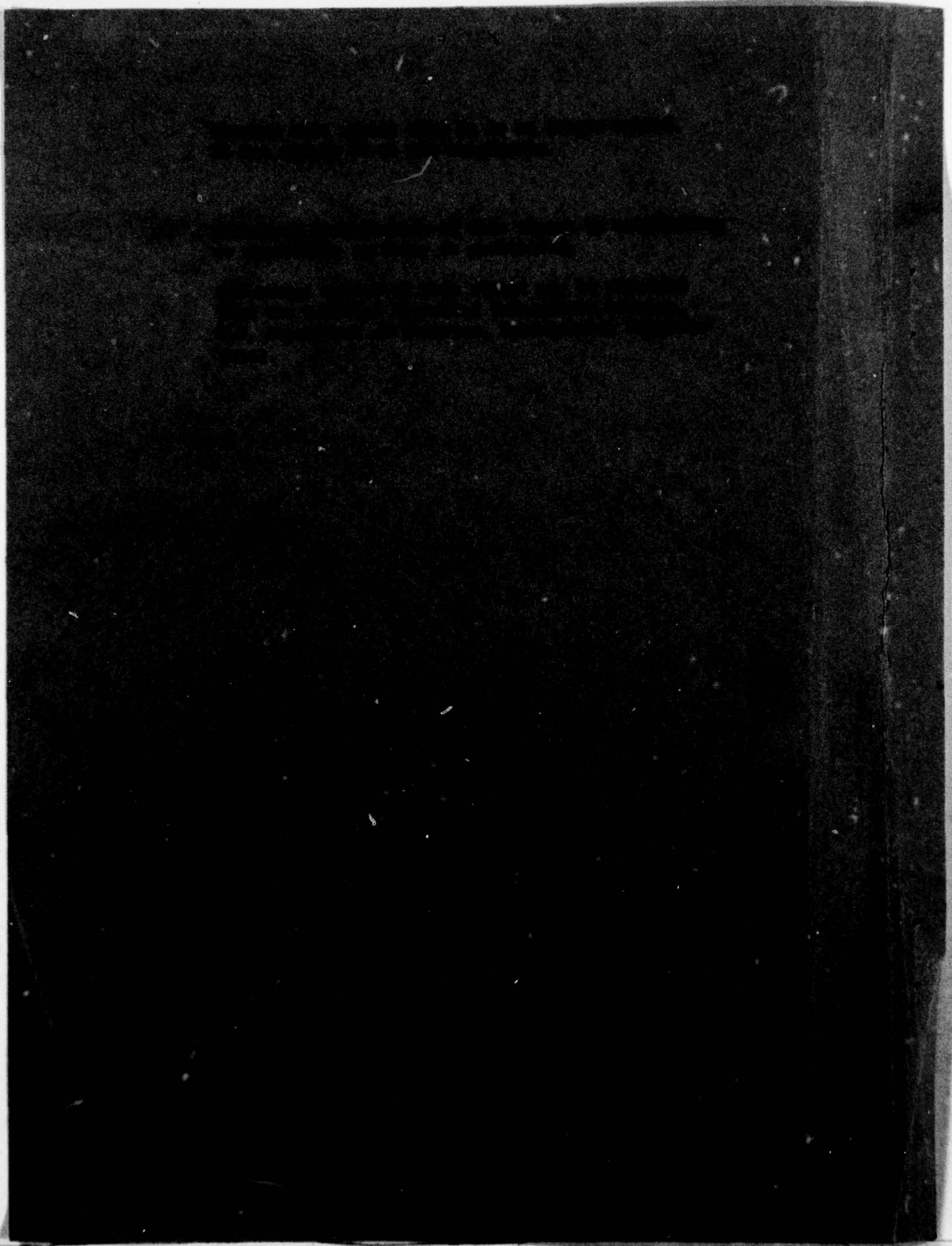
AD A 050309

REPORT NO. 2021

COHERENCE RETENTION DURING ROTATIONALLY
INELASTIC COLLISIONS OF SELECTIVELY
EXCITED DIATOMIC MOLECULES

THE A. C. ...
... ..

DDC
RECEIVED
FEB 23 1978
B



UNCLASSIFIED

SECURITY CLASSIFICATION OF THIS PAGE (When Data Entered)

REPORT DOCUMENTATION PAGE		READ INSTRUCTIONS BEFORE COMPLETING FORM
1. REPORT NUMBER BRL Report No. 2021	2. GOVT ACCESSION NO. BRL-2021	3. RECIPIENT'S CATALOG NUMBER
4. TITLE (and Subtitle) COHERENCE RETENTION DURING ROTATIONALLY INELASTIC COLLISIONS OF SELECTIVELY EXCITED DIATOMIC SULFUR		5. TYPE OF REPORT & PERIOD COVERED
7. AUTHOR(s) Thomas A/ Caughey David R/ Crosley		6. PERFORMING ORG. REPORT NUMBER
9. PERFORMING ORGANIZATION NAME AND ADDRESS US Army Ballistic Research Laboratory Aberdeen Proving Ground, Maryland 21005		8. CONTRACT OR GRANT NUMBER(s)
11. CONTROLLING OFFICE NAME AND ADDRESS US Army Materiel Development & Readiness Command 5001 Eisenhower Avenue Alexandria, Virginia 22333		10. PROGRAM ELEMENT, PROJECT, TASK AREA & WORK UNIT NUMBERS RDTC 11L161102AH43
14. MONITORING AGENCY NAME & ADDRESS (if different from Controlling Office)		12. REPORT DATE OCT 1977
		13. NUMBER OF PAGES 35
		15. SECURITY CLASS. (of this report) Unclassified
16. DISTRIBUTION STATEMENT (of this Report) Approved for public release; distribution unlimited.		16a. DECLASSIFICATION/DOWNGRADING SCHEDULE
17. DISTRIBUTION STATEMENT (of the abstract entered in Block 20, if different from Report)		
18. SUPPLEMENTARY NOTES *Department of Chemistry, University of Wisconsin, Madison, WI 53706		
19. KEY WORDS (Continue on reverse side if necessary and identify by block number) Coherence retention Rotationally inelastic collisions Hanle effect Diatomic sulfur		
20. ABSTRACT (Continue on reverse side if necessary and identify by block number) (81) Hanle effect broadening rates have been measured for diatomic sulfur, selectively excited to the $v=4, N=40, J=41$ level of the electronically excited B (triplet sigma) state, with a variety of collision partners. In the cases of diatomic nitrogen and the rare gases, a comparison with previously determined rotational and vibrational energy transfer rates shows that coherence is retained throughout transfer collisions. This is confirmed by direct observation of the Hanle effect in nearby rotational levels populated by collision, using a monochromator (Contd)		

DDC
RECEIVED
FEB 23 1978
B

050 7501

Jeh

UNCLASSIFIED

SECURITY CLASSIFICATION OF THIS PAGE(When Data Entered)

Item 20, Continued:

to disperse the fluorescence. These results indicate that collisions which change the magnitude of the rotational angular momentum (even by several quanta) do not severely alter its orientation.

RECEIVED
FEB 28 1978
D D C

UNCLASSIFIED

SECURITY CLASSIFICATION OF THIS PAGE(When Data Entered)

TABLE OF CONTENTS

	Page
LIST OF ILLUSTRATIONS.	5
LIST OF TABLES	7
INTRODUCTION	9
EXPERIMENTAL	12
BROADBAND EXPERIMENTS.	13
NARROWBAND EXPERIMENTS	19
DISCUSSION	24
CONCLUSIONS.	28
ACKNOWLEDGEMENT.	29
REFERENCES	30
APPENDIX A. PHASE-SENSITIVE DETECTION CORRECTIONS	32
DISTRIBUTION LIST.	35

BLANK PAGE

ACCESSION for		
NTIS	White Section	<input checked="" type="checkbox"/>
DDC	Blue Section	<input type="checkbox"/>
UNANNOUNCED		<input type="checkbox"/>
JUSTIFICATION		
BY		
DISTRIBUTION/AVAILABILITY CODES		
Dist.	AVAIL	SPECIAL
A		

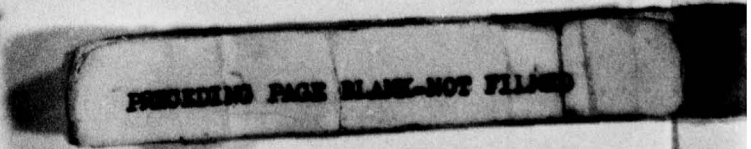
LIST OF ILLUSTRATIONS

Figure	Page
1. Full-width at half maximum (FWHM) of the broadband Hanle effect signal as a function of S_2 number density. Error bars are from linefit confidence limits; those at the lowest pressures have been omitted for clarity but are of a similar size. The solid line is a least-squares fit to the data, and the shaded region is the broadening prediction assuming $k_{cd} = k_Q$	15
2a. Broadband Hanle effect signal (FWHM) as a function of He number density. The solid line is a least squares fit. The shaded area is the broadening predicted by Eq. (1) using previously determined k_R , k_V and k_Q	16
2b. Broadband Hanle effect signal (FWHM) as a function of Xe number density. The solid line is a least squares fit. The shaded area is the broadening predicted by Eq. (1) using previously determined k_R , k_V and k_Q	17
3. Hanle effect signals - lock-in amplifier output. (a) Broadband experiment with no added gas, (b) 'Transfer' signal using monochromator	20
4. Hanle effect signal widths in He. Open circles are experimental results. Solid circles are results of simulations. The shaded area is the prediction assuming no coherence retention. (a) Narrowband runs ('transfer' signals only). (b) Broadband runs ('transfer' signals plus initially pumped level signal).	22
5. Form of the transfer signals for an F_1 , an F_2 , and an F_3 level each with the same value of \bar{g} , τ and degree of polarization.	26

LIST OF TABLES

Table	Page
1. Broadband Experimental Results. Effective broadening cross sections σ_{cd} , and energy transfer cross sections from Ref. 9. All units are \AA^2	18
2. Widths (in G) of Hanle effect signals at 2.35 Torr He	23
3. Case (b) g-values for a $^3\Sigma$ state with rotational quantum number N.	23

BLANK PAGE



INTRODUCTION

There is ample experimental evidence for the presence of non-equilibrium population distributions, and the occurrence of non-Arrhenius reaction rate behavior, in a wide variety of combustion processes. A full understanding of such systems on a microscopic level requires that such effects be addressed. Recent experiments are now just beginning to provide information on the detailed quantum level dependence of inelastic and reactive collisions for a number of small molecules. However, the difficulty involved in carrying out such experiments means that theoretical computations of such rates will continue to be important for a number of systems. It is in turn crucial to have at hand experimental evidence concerning details of the collision dynamics which place constraints upon the theoretical formulations.

An important aspect of such computations is the detailed m_j dependence of reactive and inelastic collision cross sections.¹ Most of the experimental evidence comes from molecular beam work on oriented molecules² but the use of laser excited fluorescence techniques promises³ further new data on a larger class of molecules. Computations describing reactive beam experiments have been made in the statistical limit,⁴ and for inelastic collisions under conditions of weak and strong coupling of the collisional angular momentum, with a view toward laser-excited fluorescence experiments.⁵

An important practical consideration for trajectory calculations is indeed the choice of angular momenta coupling.^{5,6} Accordingly, it is important to have experimental evidence for the correlation^{4,7} of the angular momentum observables during a collisional encounter (or, for that matter, correlation between any sets of observables is most useful⁸).

¹J. P. Toennies, "The Calculation and Measurement of Cross Sections for Rotational and Vibrational Excitation," *Ann. Rev. Phys. Chem.* **27**, 225-260 (1976).

²P. R. Brooks, "Reactions of Oriented Molecules," *Science* **193**, 11-16 (1976).

³B. E. Wilcomb and P. J. Dagdigian, "Electric Quadrupole State Selection with a Laser Fluorescence Detector," Paper RC9, Symposium on Molecular Spectroscopy, Columbus, Ohio, June 1977.

⁴D. A. Case and D. R. Herschbach, "Statistical Theory of Angular Momentum Polarization in Chemical Reactions," *Mol. Phys.* **30**, 1537-1564 (1975); "Statistical Theory of Angular Distributions and Rotational Orientation in Chemical Reactions," *J. Chem. Phys.* **64**, 4212-4222 (1976).

⁵M. H. Alexander and P. J. Dagdigian, "Rotational Alignment in Inelastic Collisions," *J. Chem. Phys.* **66**, 4126-4132 (1977).

⁶T. F. George, University of Rochester, private communication, 1977.

⁷D. R. Herschbach, "Molecular Beam Studies of some Elementary Oxidation and Flame Reactions," 16th Symposium on Combustion, Cambridge, Mass., August 1976, Book of Abstracts, pp. 159-160.

⁸R. D. Levine, Hebrew University, private communication, 1977.

In the course of our investigation⁹ of relaxation within the $B^3\Sigma_u^-$ state of the S_2 molecule, induced by collisions with a variety of gases, we have studied the effects of collisions on the Hanle effect signals. While these results do not provide a full set of correlation data, they do indeed furnish the type of input useful for theoretical computations such as those discussed above.

The Hanle effect, or zero-field level crossing, is caused by the establishment of coherence among excited state m_j levels. This is achieved by the choice of polarization of the exciting radiation, and is observed through the change in the polarization of the resulting fluorescence upon application of a magnetic field.¹⁰ Through a suitable basis set rotation, the existence of coherence may also be regarded as indicating a particular direction, with respect to some space-fixed axis, of the precessing J-vector. The essential result of the current study is that after collisions which transfer the selectively excited S_2 to nearby rotational levels, a high degree of coherence is maintained. This means that collisions which change the value of the rotational quantum number do not severely alter its direction in space. Together with our results⁹ on relative rates of transfer to different triplet components, these data place stringent requirements on theoretical descriptions of the angular momentum changes accompanying rotationally inelastic collisions.

Using a somewhat different technique, Katô *et al.*¹¹ have quite recently measured orientational persistence during rotationally and vibrationally inelastic collisions of selectively excited $B^3\Pi_{ou}^+ I_2$. We shall not comment here further on a comparison of their findings¹² and ours except to note that those authors and ourselves were both surprised at the high degree of retention found in the respective investigations. Non-zero polarization of light emitted by levels populated by rotational transfer collisions has been noted¹² in Li_2 , while Lengel's observations¹³

⁹T. A. Caughey and D. R. Crosley, "Relaxation in the $B^3\Sigma_u^-$ State of S_2 . II. Rotational," to be published.

¹⁰R. N. Zare, "Interference Effects in Molecular Fluorescence," *Acc. Chem. Res.* **4**, 361-367 (1971).

¹¹H. Katô, R. Clark and A. J. McCaffery, "Rotational Assignments in Excited Iodine and Reorientation by Elastic and Inelastic Collisions from Circularly Polarized Emission," *Mol. Phys.* **31**, 943-956 (1976); H. Katô, S. R. Jeyes, A. J. McCaffery and M. D. Rowe, "Persistence of m_j Following Vibrational and Rotational Energy Transfer in Molecular Iodine Excited by a Single Mode Tunable Dye Laser," *Chem. Phys. Letters* **39**, 573-575 (1976).

¹²Ch. Ottinger, R. Velasco and R. N. Zare, "Some Propensity Rules in Collision-Induced Rotational Quantum Jumps," *J. Chem. Phys.* **52**, 1636-1643 (1970).

¹³R. K. Lengel and D. R. Crosley, unpublished data.

on OH indicated little or no coherence retention in that molecule. Results¹⁴ on rotational transfer in Na₂ have shown that significant depolarization during rotationally inelastic collisions occurs only for low rotational levels and the heavier rare gases. Studies of atomic systems have demonstrated such retention for both interatomic transfer ('sensitized fluorescence')¹⁵ and intraatomic transfer.¹⁶ While no general trends concerning coherence retention are yet discernible, these studies are suggestive enough to encourage further experimental inquiries, as well as an examination of theoretical models as regards the orientational memory.

It should be noted that, properly, our experiment establishes and measures the relaxation of the alignment (a quadrupolar distribution of population over the m_j levels) and not orientation (a dipolar distribution). However, the relaxation times for these two tensor components of the density matrix describing the excited state are related to one another;¹⁷ for the case of collisions with a foreign gas, they differ by twelve percent.¹⁸ Consequently, we view the phenomena as more or less interchangeable, i.e., the retention of coherence in the Hanle effect experiment yields, in a directly calculable way, results applicable to the relaxation of the orientation of the angular momentum vector.

¹⁴K. Bergmann and W. Demtröder, "Inelastic Collision Cross Section of Excited Molecules. II. Asymmetries in the Cross Section for Rotational Transitions in the Na₂ ($B^1\Pi_u$) State," J. Phys. B 5, 1386-1395 (1972).

¹⁵W. Gough, "The Polarization of Sensitized Fluorescence," Proc. Phys. Soc. London 90, 287-296 (1967).

¹⁶M. Elbel, B. Niewitecka and L. Krause, "Coherence Transfer Between the $^2P_{1/2}$ and $^2P_{3/2}$ States in Sodium, Induced in Collisions with Helium Atoms," Can. J. Phys. 48, 2996-3003 (1970).

¹⁷A. Omont, "Resolution of the Density Operator into Irreducible Tensor Components and Applications to Experiment," in P. G. H. Sandars, ed., Atomic Physics II: Proceedings of the Second International Conference, Oxford, 1970 (Plenum, 1971), pp. 191-200.

¹⁸P. R. Berman and W. E. Lamb, Jr., "Influence of Foreign Gas and Resonant Collisions on Line Shapes," Phys. Rev. 187, 221-266 (1969).

EXPERIMENTAL

The basic experimental apparatus¹⁹ has been previously described.* The modifications are the use of a refillable cell,⁹ and, in some experiments, a 3/4-m spectrometer to disperse the fluorescence. Briefly, light from an atomic zinc line source is focussed into a quartz cell containing sulfur. The cell is connected to a high vacuum line for filling with collision partner gases, whose pressure is measured by an NRC Alphatron gauge. The S₂ pressure is controlled by the temperature of a sidearm reservoir; the ambient temperature of the experiment is about 900 K. The Zn 307.6 nm line excites the v' = 4, N' = 40, J' = 41 level of the B³Σ_u⁻ state.¹⁹ Fluorescence from this level (and/or nearby ones populated by collisions, for non-zero fill gas pressures) is detected at right angles by a photomultiplier after passing through either filters or the spectrometer. A slowly varying magnetic field is applied to the cell for observation of the Hanle effect, while a smaller AC field permits the use of lock-in detection. The result, plotted on an xy-recorder, is a signal resembling the derivative of a Lorentzian; in actuality it is modulation broadened and possibly modified in shape as well as breadth due to collisional processes.

The results are manually digitized and fit by a non-linear regression routine to a single modulation-broadened Lorentzian using Wahlquist's closed-form expression.²² Although the actual signal can be a composite of Lorentzian and non-Lorentzian curves, the signal-to-noise ratios involved render this characterization adequate. Our model calculations necessary for interpretation of the results (see below) are also cast in the form of a best-single-Lorentzian representation for comparison purposes. All widths given in the paper refer to the full width at half maximum of the true or equivalent Lorentzian curve.

* The lifetimes (~ 20 nsec for J' ~ 40 in v' = 3 and 4) of ref. 19 are incorrect by about a factor of two due to the presence of an as yet unidentified quenching gas present in the cell used. The new measurements,²⁰ which employ the re-evacuatable cell used in the present work, also indicate however that the lifetime of J' = 13, v' = 4 is ~ 20 nsec. Which of these values, if either, is truly characteristic of v' = 4 is not yet understood,²¹ although this problem should not affect the results described here.

¹⁹ K. A. Meyer and D. R. Crosley, "Hanle Effect Lifetime Measurements on Selectively Excited Diatomic Sulfur," J. Chem. Phys. 59, 1933-1941 (1973).

²⁰ T. A. Caughey, K. A. Meyer and D. R. Crosley, "Lifetimes in the B³Σ_u⁻ State of S₂," to be published.

²¹ K. A. Meyer, "Some Radiative Properties of the B³Σ_u⁻ State of Diatomic Sulfur," Ph.D. thesis, University of Wisconsin, 1976.

²² H. Wahlquist, "Modulation Broadening of Unsaturated Lorentzian Lines," J. Chem. Phys. 35, 1708-1710 (1961).

BROADBAND EXPERIMENTS

For a single emitting level, under the conditions of the right angle geometry we employ, the Hanle effect appears as an inverted Lorentzian dependence of intensity upon magnetic field H , centered at $H = 0$. The breadth of the Lorentzian is inversely proportional to the product of the magnetogyric ratio g and effective lifetime τ of the coherence in the emitting state. τ , in turn, is the inverse of the sum of all rates responsible for destruction of the coherence, which include radiation and collisions. This collisional coherence destruction rate for a single collision partner may be written as a product of the number density n and a coherence destruction rate constant, k_{cd} .

For current purposes, the collisional fate of a selectively excited S_2 molecule may be divided into four qualitatively distinct categories. These and their associated rate constants are: electronic quenching[†] (k_Q); vibrational transfer (k_V); rotational transfer (k_R); and depolarization (k_D). This last type of collision, which leaves the S_2 in the same quantum level but destroys the coherence, may also be viewed as elastic reorientation. Under the assumption that all inelastic collisions result in a destruction of the coherence, k_{cd} would be the sum of these rates,

$$k_{cd} = k_Q + k_V + k_R + k_D; \quad (1)$$

whereas a lack of equality in the measured rates would imply that coherence is retained during an energy transfer process.

Our studies⁹ of quenching and energy transfer show that the collision partners investigated form two manifest types. Collisions of excited S_2 molecules with ground-state S_2 , with SO_2 , or with H_2S lead primarily to quenching of the fluorescence, i.e., for these molecules, $k_Q \gg k_V, k_R$. For the rare gases or N_2 as a collision partner, on the other hand, the dispersed fluorescence shows many features due to vibrationally and rotationally relaxed B-state S_2 ; here, $k_R > k_V \gg k_Q$.

* Ground-state S_2 is of course present as a potential collision partner in all the experiments. Its (separately measured) influence on results with other fill gases has been removed in the analysis and will be ignored in the equations for reasons of simplification.

† Including both reactive and non-reactive quenching, between which our experiment cannot distinguish.

The first series of experiments involve the measurement of the Hanle effect broadening rate using a broad-band filter (two Corning 7-54's) passing fluorescence from the initially pumped level as well as others populated by rotationally and vibrationally inelastic collisions. For those gases in which quenching dominates, nearly all of the fluorescence will emanate from the initially pumped level, and a single collision broadened Lorentzian should yield an accurate fit to the data. The results for collisions with ground state S_2 are shown in Fig. 1. Plotted, as a function of S_2 number density, are the Hanle effect widths; the error bars result from the confidence limits on the fit to the experimental data. Also included is a predicted curve based on the assumption $k_Q \gg k_V, k_R, k_D$ so that $k_{cd} = k_Q$. The previous investigation⁹ of the variation of fluorescence intensity with sulfur pressure furnishes the quenching rate* for $S_2(B) - S_2(X)$ collisions, $k_Q = (13 \pm 3) \times 10^{-10} \text{ cm}^3 \text{ sec}^{-1}$, as well as demonstrating that $k_Q \gg k_V, k_R$. The agreement between prediction and experiment shows that $k_Q \gg k_D$ also, i.e., that quenching dominates the entire collision process, and is faster than not only rotational or vibrational transfer, but the elastic reorientation process as well. In Table 1 are listed the cross sections, which are seen to overlap to within experimental error.

Hanle effect broadening rates have also been measured for H_2S and SO_2 , and the cross sections are included in Table 1. In view of our prior observations that, for these gases, $k_V, k_R \ll k_Q$, and under the assumption that here also $k_D \ll k_Q$, these cross sections provide a measure of the quenching efficiency of these gases.

A contrasting picture is presented by nitrogen and rare gas collision partners, as is illustrated in Fig. 2 for the cases of helium and xenon. Again the experimental widths are plotted along with the broadening predicted by the assumption of Eq. (1). We use in Eq. (1) our previously determined⁹ k_Q, k_V and k_R , and take, for lack of information, $k_D \ll k_R, k_V$ (a non-negligible k_D would only increase the discrepancy). We conclude that, for these gases, coherence is retained for excited S_2 molecules which have suffered rotationally (and possibly vibrationally) inelastic collisions.

A consideration of the actual contributing effects for the case of coherence retention (see below) shows that, given a noise-free signal, a single collision broadened Lorentzian is not a fully correct description of the observed broad-band signal for the rare gases and N_2 . Nevertheless, we have fit the experimental results in such a fashion, and this seems to be an adequate characterization based on the size and randomness of

* All rate constants and cross sections are calculated using a radiative lifetime of 36 nsec for $v'=4, N'=40, J'=41$.

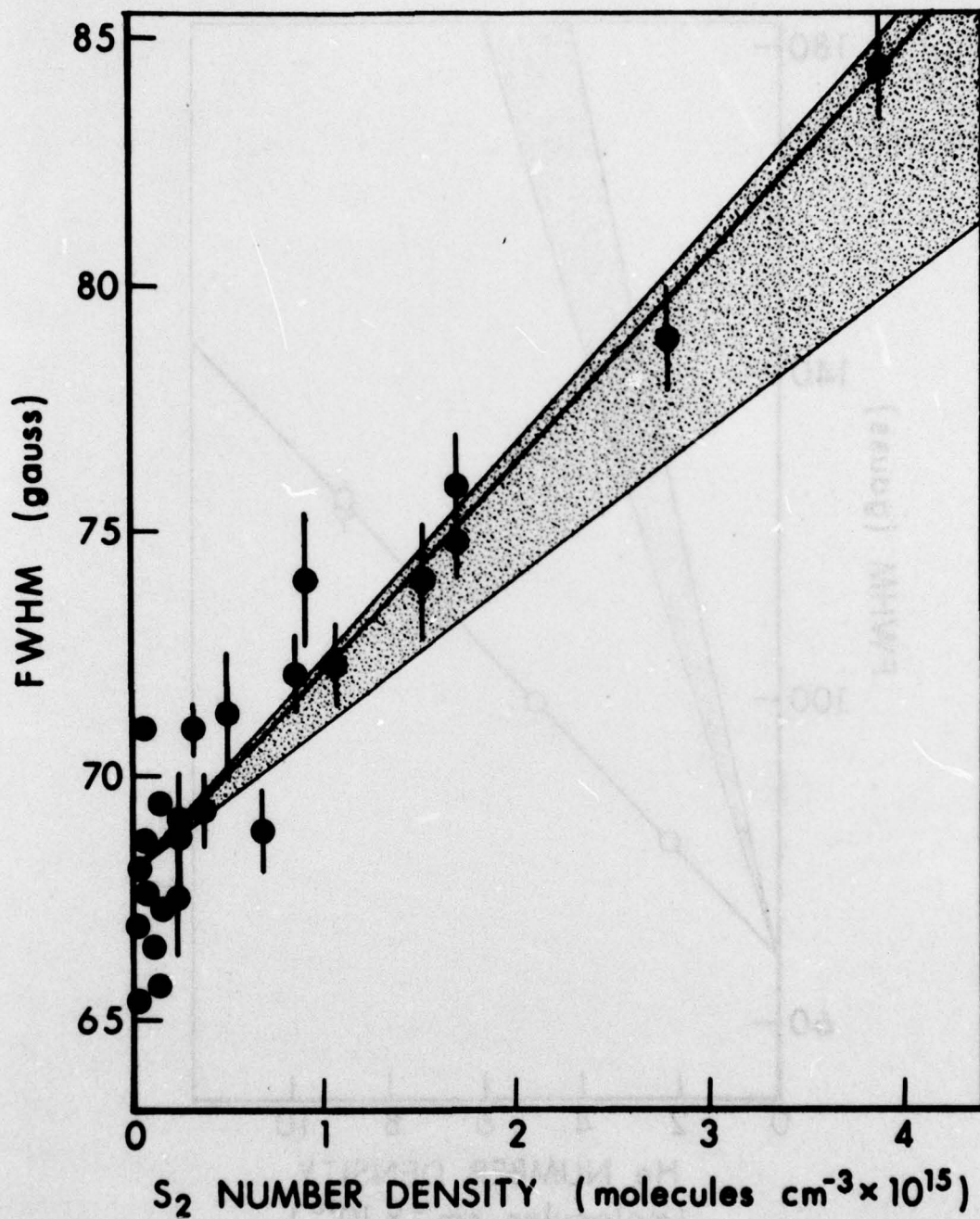


Figure 1. Full-width at half maximum (FWHM) of the broadband Hanle effect signal as a function of S_2 number density. Error bars are from linefit confidence limits; those at the lowest pressures have been omitted for clarity but are of a similar size. The solid line is a least-squares fit to the data, and the shaded region is the broadening prediction assuming $k_{cd} = k_0$.

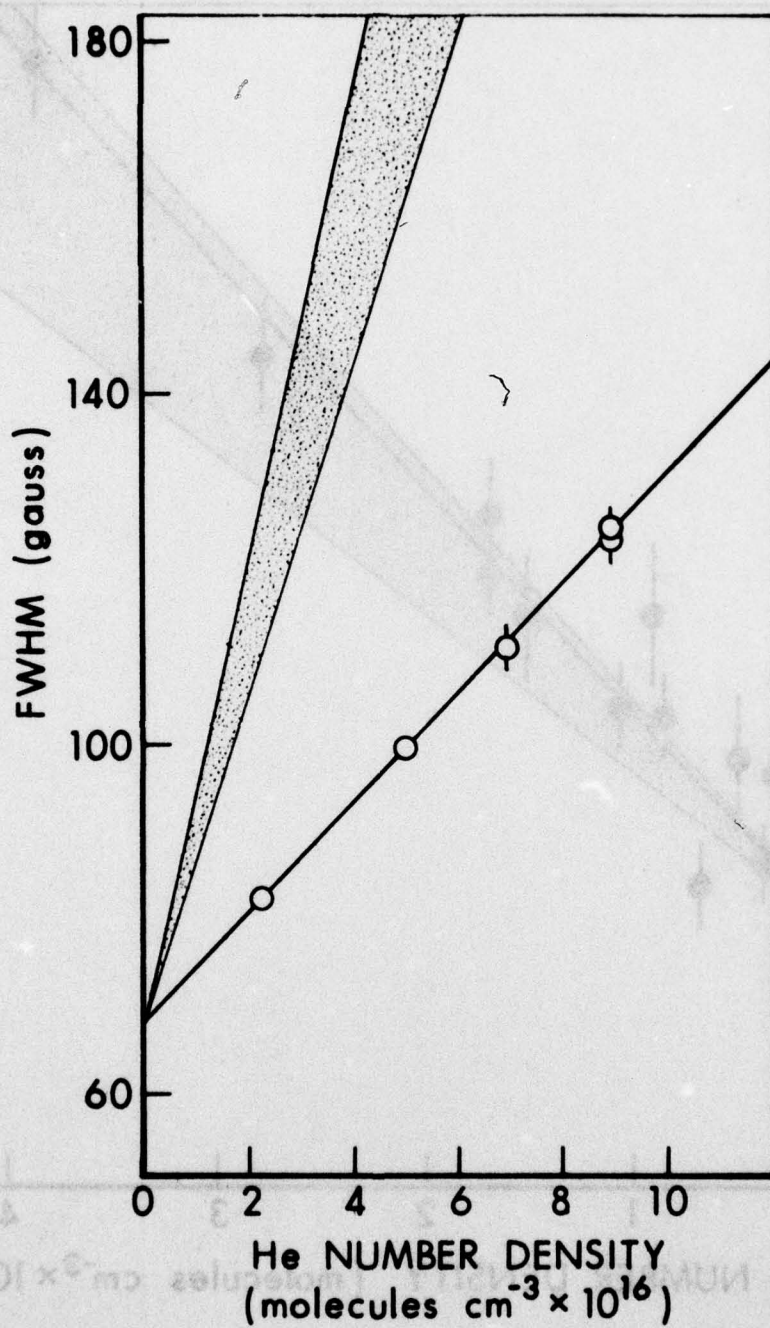


Figure 2a. Broadband Hanle effect signal (FWHM) as a function of He number density. The solid line is a least squares fit. The shaded area is the broadening predicted by Eq. (1) using previously determined k_R , k_V and k_Q .

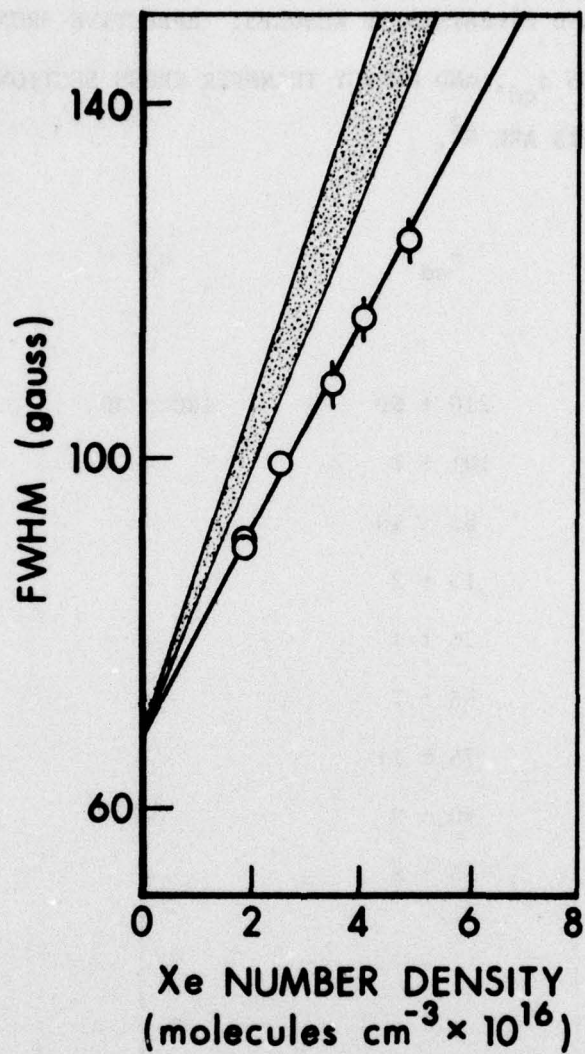


Figure 2b. Broadband Hanle effect signal (FWHM) as a function of Xe number density. The solid line is a least squares fit. The shaded area is the broadening predicted by Eq. (1) using previously determined k_R , k_V and k_Q .

TABLE 1. BROADBAND EXPERIMENTAL RESULTS: EFFECTIVE BROADENING CROSS SECTIONS σ_{cd} , AND ENERGY TRANSFER CROSS SECTIONS FROM REF. 9. ALL UNITS ARE \AA^2 .

Collision Partner	σ_{cd}	σ_Q	$\sigma_V + \sigma_R$
S ₂	210 ± 50	180 ± 40	-
SO ₂	101 ± 7	-	-
H ₂ S	82 ± 10	-	-
He	13 ± 2	-	48 ± 6
Ne	26 ± 4	-	63 ± 7
Ar	53 ± 7	-	84 ± 9
Kr	76 ± 11	-	110 ± 9
Xe	80 ± 9	-	117 ± 13
N ₂	58 ± 8	-	114 ± 16

the residuals. Also, the broadening plots, such as that shown in Fig. 2, are described quite well by a linear dependence on pressure. The observed broadening rates, analyzed in this fashion, are always less than the sum $k_V + k_R + k_Q$ for these gases. The results are presented in Table 1, as a comparison of cross-sections.

Thus, while the lifetime of the initially pumped level is shortened by rotational and vibrational state changing collisions, the lifetime of the coherence is not shortened as much. In other words, there is for these collision partners a separate, slower, rate constant for reorientation than for change in magnitude of the rotational angular momentum.

Broadband experiments have also been carried out on two other initially pumped levels deep in the $B^3\Sigma^-$ potential well ($v' = 4$, $N' = 14$, $J' = 13$ and $v' = 3$, $N' = 42$, $J' = 43$).^u The results show broadening cross sections of similar size; although σ_R and σ_V have not been measured for these levels, similar behavior is suggested. A larger broadening rate, for $S_2(B) - S_2(X)$ collisions, is found for a level near the predissociation limit ($v' = 9$; a preliminary analysis yields $N' = 22$, $J' = 23$), possibly indicating collision-induced dissociation.

NARROWBAND EXPERIMENTS

If coherence is retained throughout a rotationally inelastic collision, then Hanle effects should be observable in the fluorescence emitted by rotationally transferred molecules. In this series of experiments, where He and Xe are the collision partners, a 3/4-m spectrometer was used to disperse the fluorescence before detection. With a typical operating entrance/exit slit width of 500/1000 μ in second order, the bandpass is a trapezoid with a 75 cm^{-1} base and 25 cm^{-1} top (full widths in first order). With the monochromator set 51 cm^{-1} from the nearest line ($R_1(39)$) emitted by the initially pumped level, the detector views fluorescence emitted by levels ranging approximately* from $N' = 10$ to $N' = 34$ of $v' = 4$.

Fig. 3 shows the Hanle effect signal observed under these conditions and at a pressure of 0.72 Torr helium ($2.33 \times 10^{16} \text{ cm}^{-3}$), using field modulation and lock-in amplifier techniques. (We shall find it useful to refer below to this as the 'transferred signal'.) Also shown is the Hanle effect signal using broadband detection, but with no added gas, so that only the initially pumped level is emitting. It was verified that no transferred signal appeared when: (i) the fill gas was pumped out of the cell; (ii) only fluorescence polarized parallel to H was detected; or (iii) the reservoir was cooled so as to condense the sulfur from the cell. These experiments provide conclusive evidence that coherence is retained throughout rotational energy transfer collisions.

*The actual range depends on the triplet component involved; also some levels emit only part of their rotational branch structure within this bandpass. The true distribution is used in the simulation described below.

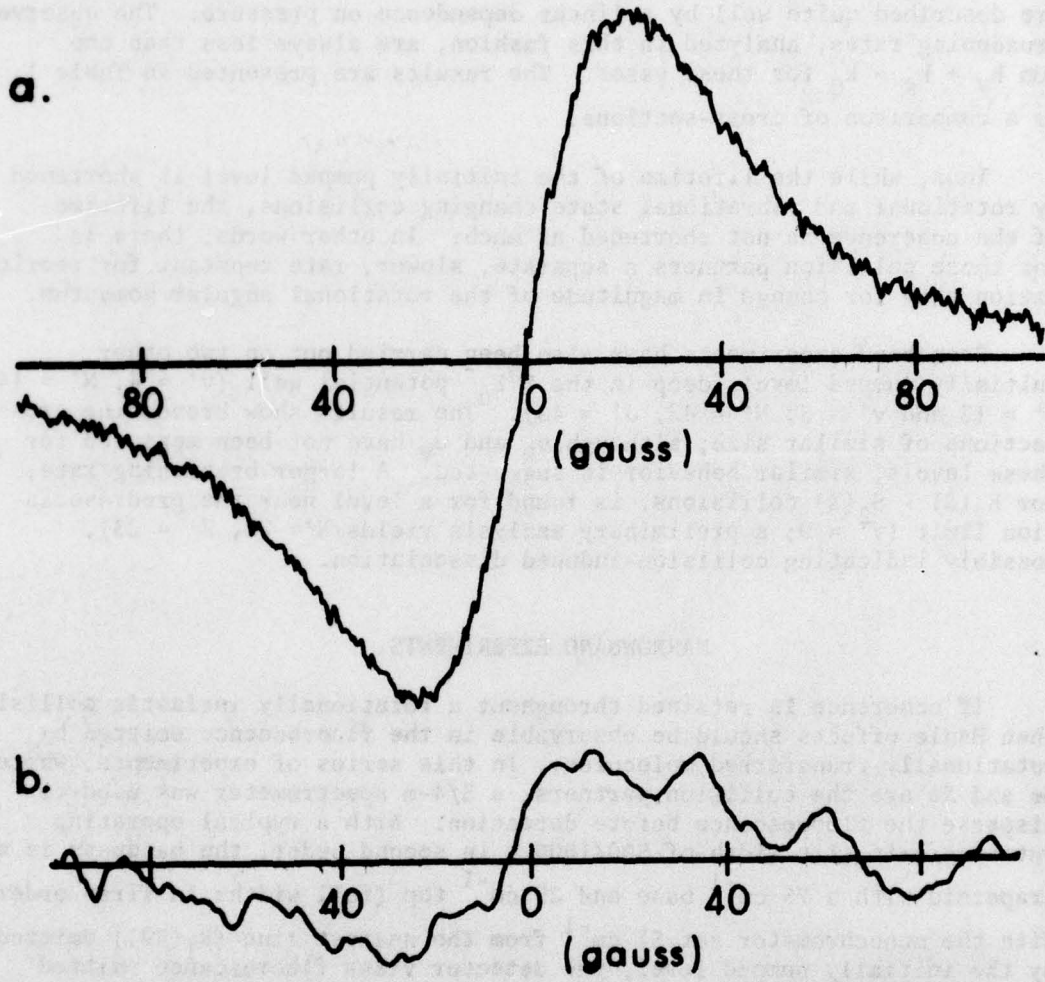


Figure 3. Hanle effect signals - lock-in amplifier output. (a) Broadband experiment with no added gas, (b) 'Transfer' signal using monochromator.

Information is provided by both the amplitude and the breadth of the transferred signals, as delineated more fully in the discussion section. Amplitudes have been measured for both He and Xe, and the width studied as a function of He pressure. The widths are characterized by (i.e., fitted to) a single modulation-broadened Lorentzian; we repeat that while this is not the correct form, it is an adequate representation for our purposes. The resulting widths for the narrowband runs, as a function of He number density, are plotted in Fig. 4; the error bars are obtained from the confidence limits on the fitting procedure.

The important feature of the data exhibited in Fig. 4 is that the widths are significantly narrower than those obtained in the broadband runs. The reason for this is that the transferred signals are a different shape, and appear narrower, particularly with the mode of detection used (see below).

In contrast, the Hanle effect detected in light emitted by the initially pumped level only should remain a true Lorentzian, with a broadening given by the rate constant in Eq. (1) and shown by the shaded area in Figs. 2 and 4. This is because inelastic collisions would then prevent the transferred fluorescence from reaching the detector, effectively removing (at the collision rate) the coherence together with the emission. The broadband experiments thus involve a composite of the narrow transferred signals and a broad Lorentzian due to the initially pumped level, and their breadths fall between the narrowband runs and the predictions of Eq. (1). If the monochromator is tuned to the lines emitted by the initially pumped levels, a broad signal should result. This experiment was carried out at a He pressure of 2.35 Torr. However, underlying the lines emitted by the initially pumped level, and thus within the bandpass of the monochromator, is some fluorescence emitted from molecules which have undergone rotational energy transfer. Thus this signal too should be a composite, but weighted more heavily in favor of the broad component. The results at 2.35 Torr He, using these various filters, are presented in Table 2 and are ordered according to expectations.

Transferred signals were searched for in the fluorescence emitted by vibrationally transferred molecules ($v' = 4 \rightarrow v' = 3$) using the monochromator. However, since $k_V < k_R$, a poorer signal to noise ratio was obtained compared to the case of observation of rotationally transferred molecules. Even in the case of complete coherence retention during a vibrationally inelastic collision, the resulting amplitude of the transferred signal would have been below our level of detectability by a factor of about 1.5. Hence we have no direct evidence for the presence or absence of coherence retention during such collisions. Nor do the broadband experiments furnish any information on this point, since $k_{cd} > k_V$ in all cases.

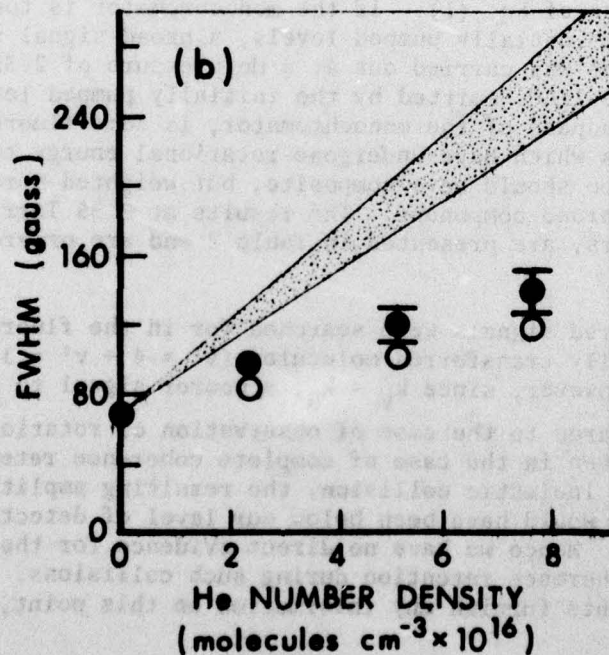
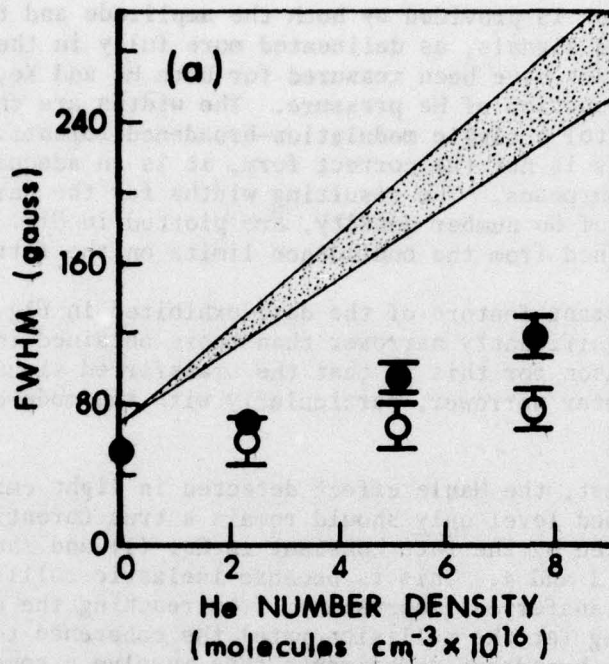


Figure 4. Hanle effect signal widths in He. Open circles are experimental results. Solid circles are results of simulations. The shaded area is the prediction assuming no coherence retention. (a) Narrowband runs ('transfer' signals only). (b) Broadband runs ('transfer' signals plus initially pumped level signal).

TABLE 2. WIDTHS (IN G) OF HANLE EFFECT SIGNALS AT 2.35 TORR He.

conditions	width
narrowband, transferred	80 ± 10
broadband	125 ± 10
narrowband, initially pumped	190 ± 30
predicted, Eq. (1)	260 ± 25

TABLE 3. CASE (b) g-VALUES FOR A $^3\Sigma$ STATE WITH ROTATIONAL QUANTUM NUMBER N.

Level Designation	J	g_J
F_1	$N + 1$	$- 2/(N + 1)$
F_2	N	$- 2/N(N + 1)$
F_3	$N - 1$	$2/N$

DISCUSSION

A classical picture of Hanle effects in transferred molecules, as presented by Bayliss²³ (an alternate derivation is given by Chiu²⁴) for a single collision, two level system, forms the basis for understanding and analyzing the results of the preceding section. Bayliss shows that fluorescence emitted by molecules which have undergone an inelastic collision will, for right angle geometry, exhibit a field dependence of the intensity I having the form:

$$I \propto 1 + \frac{\beta_1 \beta_2 - 1}{(1 + \beta_1^2)(1 + \beta_2^2)} \quad (2)$$

Here, $\beta_i = 2g_i \mu_0 \tau H/\hbar$; μ_0 is the Bohr magneton and \hbar is the Dirac constant. The lifetime* τ is the inverse of the sum of all rates for the loss of coherence from a single level, i.e.,

$$\tau^{-1} = \tau_r^{-1} + (k_Q + k_V + k_R + k_D)n \quad (3)$$

where τ_r is the radiative lifetime.

The $B^3\Sigma_u^-$ state of the S_2 molecule has three triplet components with different g -values. We use the g -values for Hund's case (b) coupling as listed in Table 3; although the triplet splitting yields slightly different magnetogyric ratios,¹⁹ these are accurate enough for our intent.

The initial excitation is to an F_1 level having $J' = 41$. In order to qualitatively examine the form of the transferred signals, we shall momentarily ignore the fact that rotationally inelastic collisions produce a change in N , i.e., we shall consider the transferred signals for transfer from an F_1 level to F_1 , F_2 and F_3 levels of the same N . Eq. (2) and the g -values of Table 3 then yield the expected appearance of the signal. Fluorescence from collisionally populated F_2 and F_3 levels shows the same field dependence as the initially excited F_1 level

* Properly, different lifetimes τ_i should be assigned to the two levels. In the absence of definite information on the topic (see, however, above) we take all lifetimes and rates to be independent of level.

²³W. E. Bayliss, "Coherence Transfer in Magnetic Fields," Phys. Rev. **7A**, 1190-1192 (1973).

²⁴L.-Y. C. Chiu, "Collisional Transfer of Coherence: Polarization of Sensitized Fluorescence," Phys. Rev. **5A**, 2053-2065 (1972).

$$I_{F_2, F_3} \propto 1 - \frac{1}{(1 + \beta^2)}, \quad (4)$$

while fluorescence from a collisionally populated F_1 level has its field dependence described by

$$I_{F_1} \propto 1 - \frac{1 - \beta^2}{(1 + \beta^2)^2}, \quad (5)$$

where the β in these simplified equations belongs to the originally populated F_1 level.

Eq. (5) represents a signal significantly narrower than that given by Eq. (4) for the same value of β ; the lineshapes are reproduced in Fig. 5. The signal vaguely resembles, but is not the same as, a Lorentzian. The physical reason why rotationally transferred F_1 molecules show a narrower signal is that the aligned magnetic dipole precesses in the same direction ($\beta_1 \approx \beta_2$) for, on the average, two lifetimes - one before the collision and one after. By contrast, the F_3 level dipoles precess in the opposite direction ($\beta_1 \approx -\beta_2$) and F_2 level dipoles precess virtually not at all ($\beta_2 \ll \beta_1$ for $J \sim 40$); both these latter cases result in no effective change in the signal shape. The narrower signal, caused by F_1 levels populated by collisions which change J but preserve the coherence, is further accentuated by the lock-in detection (see appendix). Thus it is the emission from F_1 levels which is responsible for the narrow signal observed in the monochromator experiments, and, when combined with the signal from the initially pumped level, the widths observed in the broadband runs.

In order to analyze the observed Hanle effect widths with He as a collision partner, we have calculated model data, examining the amount of coherence retention necessary to simulate our experiments. These models utilize the rotational distribution calculated from rotational transfer rates⁹ at each pressure, together with the spectral bandpass appropriate to the experiment. Multi-quantum rotational transfer can occur upon a single collision (we have observed up to $\Delta J \sim 14$ in collisions with He), as well as by sequential collisions; it was necessary to take into account S_2 molecules which have suffered as many as three rotationally inelastic² collisions. This was done using measured⁹ overall and relative ($F_i \rightarrow F_j$) transfer rates, and extending Eq. (2) to include sequential collisions. Effects of the modulation field on the width of the transferred signal are not negligible, and were included as described in the appendix. It is assumed that no coherence is retained in vibrationally inelastic collisions; this is immaterial for the narrow-band run simulations (no $v' = 3$ or 5 emission enters the detector), and, because $k_V < k_R$, not crucial for the broadband experiments at the low He pressures modelled.

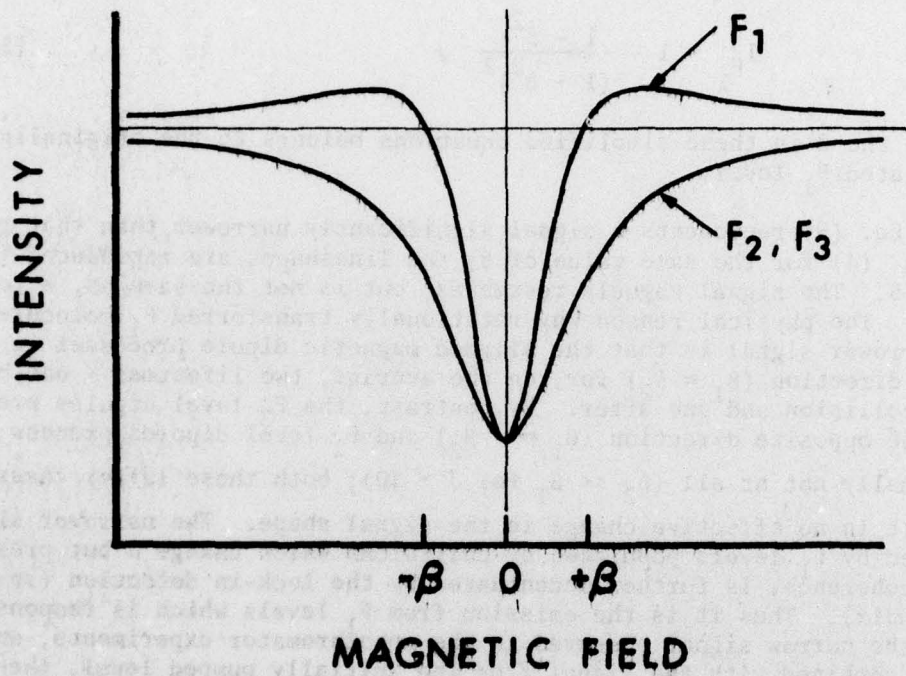


Figure 5. Form of the transfer signals for an F_1 , an F_2 , and an F_3 level each with the same value of g , τ and degree of polarization.

Curves resulting from Eq. (2) were calculated for each triplet component (F_1 , F_2 , or F_3) using the average value of J populated respectively by one, two, or three collisions. These were then weighted by the appropriate relative populations, and summed to yield a single model curve. This was in turn fit to the form of a single modulation-broadened Lorentzian for comparison with experiment.

The only adjustable parameter in the calculation is the degree of retention of coherence in each single collision. Only with a high degree of coherence retention are we able to reproduce, in the model, the experimental results; the best agreement with experiment is obtained by choosing full retention of coherence for all rotationally inelastic collisions. The calculated broadening curves are given in Fig. 4 for the broadband and monochromator runs, together with the experimental data. The broadband run simulations are obtained by combining the transferred-level Hanle effect curves, and a single modulation-broadened Lorentzian to represent the pumped level.

Model data have also been calculated assuming full coherence retention in $F_1 \rightarrow F_1$ transfer collisions, but no retention in transfer to F_2 and F_3 levels. With this assumption the calculated broadband widths are considerably broader than the experimental curves. While the best agreement between models and experiments is less sensitive to the degree of retention in $F_1 \rightarrow F_2, F_3$ collisions, it is clear that at least some coherence is retained in such encounters which change both the magnitude of the rotational angular momentum and the spin projection upon the J -vector.

The overall results of the width simulations thus indicate that a high degree of coherence is retained in all the rotational transfer collisions. For 100% retention, the narrowband data are still slightly narrower than the simulations; this may be due to some uncertainty in the rotational distribution, as projected from our measured rate constants, particularly for levels having small final values of J (≤ 25). (The larger g -value for levels with smaller J would lead to a narrower transferred signal. If any levels of lower J have, however, a shorter lifetime, that would increase the discrepancy. The degree of polarization of the fluorescent lines, for a given degree of coherence, should not change enough¹⁹ with decreasing J to affect the results.)

Given that there exists a high degree of retention, so that the form of the signal is established, the model may be used to extract a more quantitative result for the degree of coherence retention. From the lock-in amplifier peak-to-peak amplitude (see Fig. 3) and total fluorescence intensity observed in the narrow-band runs at 0.72 torr of He, the field dependence* of the transferred signal (see Fig. 5) is $3.1 \pm 0.4\%$.

* I.e., the fractional difference in signal caused by switching H from zero to a very high value.

This corresponds to a single-collision coherence retention fraction of 0.85 ± 0.15 . It is in agreement with the width simulations in that it is large, approaching complete retention. This fraction decreases with increasing mass of the rare gas collision partner: for Xe, a coherence retention fraction of 0.40 ± 0.10 was obtained. (While the poorer signal to noise ratio precluded quantitative narrowband width measurements and simulations for Xe, qualitative examination of the widths are in accord with this result.)

These values are consistent with the comparison of broadband experimental broadening cross-sections to rotational and vibrational transfer cross-sections exhibited in Table 1. Although we did not make direct measurements of transferred signals using other collision partners, it is reasonable to expect that the degree of coherence retention will scale with the ratios given there.

CONCLUSIONS

The direct observation of the Hanle effect, in fluorescence emitted by S_2 molecules which have suffered rotationally inelastic collisions with He or Xe, unambiguously demonstrates that coherence is retained throughout such collisions. This is consistent with the finding, using broadband detection, that the coherence lifetime is significantly longer than the collisional lifetime of the initially pumped level, for all the rare gases and N_2 as collision partners. In contrast, quenching dominates collisions of excited S_2 with ground state S_2 ; here the lifetimes are equal within experimental error.

Simulations of the Hanle effect widths and polarizations follow Bayliss' formulation²³ of 'transferred' Hanle effect line shapes, together with modulation broadening corrections. The results of these calculations yield a single-collision coherence retention fraction of $85 \pm 15\%$ in He; this fraction decreases with increasing mass of the collision partner, becoming $40 \pm 10\%$ in Xe.

A similarly high degree of retention (75-80%) was recently found for excited I_2 - ground state I_2 collisions.¹¹ These authors used argon ion laser excitation and directly measured polarization ratios. Given adequate intensity for precise polarization measurements on dispersed fluorescence (which was not the case in our experiment), this method is, in retrospect, advantageous to Hanle effect width measurements, since it obviates the need for the models we have used to extract numerical results.

Both the results on I_2 and those of the present study show that inelastic collisions maintain a high degree of orientation of the rotational angular momentum. These findings form a requirement which should be addressed in theoretical descriptions of the collision dynamics.

ACKNOWLEDGEMENT

We thank the National Science Foundation for providing support, under Grant No. MPS74-24277, for the portion of this work performed at the University of Wisconsin.

REFERENCES

1. J. P. Toennies, "The Calculation and Measurement of Cross Sections for Rotational and Vibrational Excitation," *Ann. Rev. Phys. Chem.* 27, 225-260 (1976).
2. P. R. Brooks, "Reactions of Oriented Molecules," *Science* 193, 11-16 (1976).
3. B. E. Wilcomb and P. J. Dagdigian, "Electric Quadrupole State Selection with a Laser Fluorescence Detector," Paper RC9, Symposium on Molecular Spectroscopy, Columbus, Ohio, June 1977.
4. D. A. Case and D. R. Herschbach, "Statistical Theory of Angular Momentum Polarization in Chemical Reactions," *Mol. Phys.* 30, 1537-1564 (1975); "Statistical Theory of Angular Distributions and Rotational Orientation in Chemical Reactions," *J. Chem. Phys.* 64, 4212-4222 (1976).
5. M. H. Alexander and P. J. Dagdigian, "Rotational Alignment in Inelastic Collisions," *J. Chem. Phys.* 66, 4126-4132 (1977).
6. T. F. George, University of Rochester, private communication, 1977.
7. D. R. Herschbach, "Molecular Beam Studies of some Elementary Oxidation and Flame Reactions," 16th Symposium on Combustion, Cambridge, Mass., August 1976, Book of Abstracts, pp. 159-160.
8. R. D. Levine, Hebrew University, private communication, 1977.
9. T. A. Caughey and D. R. Crosley, "Relaxation in the $B^3\Sigma_u^-$ State of S_2 . II. Rotational," to be published.
10. R. N. Zare, "Interference Effects in Molecular Fluorescence," *Acc. Chem. Res.* 4, 361-367 (1971).
11. H. Katô, R. Clark and A. J. McCaffery, "Rotational Assignments in Excited Iodine and Reorientation by Elastic and Inelastic Collisions from Circularly Polarized Emission," *Mol. Phys.* 31, 943-956 (1976); H. Katô, S. R. Jeyes, A. J. McCaffery and M. D. Rowe, "Persistence of m_j Following Vibrational and Rotational Energy Transfer in Molecular Iodine Excited by a Single Mode Tunable Dye Laser," *Chem. Phys. Letters* 39, 573-575 (1976).
12. Ch. Ottinger, R. Velasco and R. N. Zare, "Some Propensity Rules in Collision-Induced Rotational Quantum Jumps," *J. Chem. Phys.* 52, 1636-1643 (1970).
13. R. K. Lengel and D. R. Crosley, unpublished data.

REFERENCES (CONTD)

14. K. Bergmann and W. Demtröder, "Inelastic Collision Cross Section of Excited Molecules. II. Asymmetries in the Cross Section for Rotational Transitions in the Na_2 ($B^1\Pi_u$) State," J. Phys. B 5, 1386-1395 (1972).
15. W. Gough, "The Polarization of Sensitized Fluorescence," Proc. Phys. Soc. London 90, 287-296 (1967).
16. M. Elbel, B. Niewitecka and L. Krause, "Coherence Transfer Between the $2P_{1/2}$ and $2P_{3/2}$ States in Sodium, Induced in Collisions with Helium Atoms," Can. J. Phys. 48, 2996-3003 (1970).
17. A. Omont, "Resolution of the Density Operator into Irreducible Tensor Components and Applications to Experiment," in P. G. H. Sandars, ed., Atomic Physics II: Proceedings of the Second International Conference, Oxford, 1970 (Plenum, 1971), pp. 191-200.
18. P. R. Berman and W. E. Lamb, Jr., "Influence of Foreign Gas and Resonant Collisions on Line Shapes," Phys. Rev. 187, 221-266 (1969).
19. K. A. Meyer and D. R. Crosley, "Hanle Effect Lifetime Measurements on Selectively Excited Diatomic Sulfur," J. Chem. Phys. 59, 1933-1941 (1973).
20. T. A. Caughey, K. A. Meyer and D. R. Crosley, "Lifetimes in the $B^3\Sigma_u^-$ State of S_2 ," to be published.
21. K. A. Meyer, "Some Radiative Properties of the $B^3\Sigma_u^-$ State of Diatomic Sulfur," Ph.D. thesis, University of Wisconsin, 1976.
22. H. Wahlquist, "Modulation Broadening of Unsaturated Lorentzian Lines," J. Chem. Phys. 35, 1708-1710 (1961).
23. W. E. Bayliss, "Coherence Transfer in Magnetic Fields," Phys. Rev. 7A, 1190-1192 (1973).
24. L.-Y. C. Chiu, "Collisional Transfer of Coherence: Polarization of Sensitized Fluorescence," Phys. Rev. 5A, 2053-2065 (1972).

APPENDIX A: PHASE-SENSITIVE DETECTION CORRECTIONS

We here calculate the effect of a finite modulation field upon the shape and width of the lock-in amplifier output, for the transferred Hanle effect signal described by Eq. (5),

$$I \propto 1 = \frac{1 - \beta^2}{(1 + \beta^2)^2},$$

and illustrated in Fig. 5. The signal S at a particular value of the sweep field H and small values of the modulation field $H_\omega = H_{\omega 0} \cos \omega t$ is given in terms of a Taylor series expansion as

$$S(H + H_\omega) = I(H) + I'(H)H_\omega + \frac{1}{2} I''(H)H_\omega^2 + \dots,$$

where the primes denote differentiation. Now the lock-in amplifier picks out the component proportional to $\cos \omega t$, so that its output is given by $A = \int_0^{2\pi/\omega} S(H + H_\omega) \cos \omega t dt$. Inserting the expansion $S(H + H_\omega)$ and integrating yields

$$A = \frac{H_{\omega 0} \pi}{2} \left[I' + \frac{I'' H_{\omega 0}^2}{8} + \frac{I^V H_{\omega 0}^4}{192} + \frac{I^{VII} H_{\omega 0}^6}{9216} \right];$$

even derivatives vanish, and these four terms are both necessary and adequate to describe our signals, where $H_{\omega 0}/H_c \sim 0.1$ to 0.3 ; H_c is the value of magnetic field where $I(H_c) = 0$ (see Fig. 5).

The derivatives are as follows:

$$I' = (2\beta^3 - 6\beta)/(1 + \beta^2)^3$$

$$I'' = 24(\beta^5 - 10\beta^3 + 5\beta)/(1 + \beta^2)^5$$

$$I^V = 720(\beta^7 - 21\beta^5 + 35\beta^3 - 7\beta)/(1 + \beta^2)^7$$

$$I^{VII} = 40320(\beta^9 - 36\beta^7 + 126\beta^5 - 84\beta^3 + 9\beta)/(1 + \beta^2)^9$$

Thus for the value of $H_{\omega 0}$ which we use, the signal widths will be noticeably affected by the modulation field. (Note H_c depends on the collision rate.) These equations are then used to calculate the lock-in amplifier output, whose complex shape is conveniently (but adequately) expressed in terms of a single modulation broadened Lorentzian, for comparison purposes.

It should be noted that, because of the steepness of the 'transferred' Hanle signal for small H , the lock-in amplifier output will be larger than that produced by a Lorentzian having the same values of g , τ , and degree of polarization. It is this effective accentuation of the lock-in sensitivity to the signals from the transferred levels which causes the composite (initially pumped plus transferred levels) signals to appear narrower than would be expected by simple weighting due to relative populations.

BLANK PAGE

DISTRIBUTION LIST

<u>No. of Copies</u>	<u>Organization</u>	<u>No. of Copies</u>	<u>Organization</u>
12	Commander Defense Documentation Center ATTN: DDC-TCA Cameron Station Alexandria, VA 22314	1	Commander US Army Armament Materiel Readiness Command Rock Island, IL 61201
1	Commander US Army Materiel Development and Readiness Command ATTN: DRCDMA-ST 5001 Eisenhower Avenue Alexandria, VA 22333	3	Commander US Army Armament Research and Development Command ATTN: DRDAR-LC, Dr. J. Lannon Dr. R. Field Dr. L. Harris Dover, NJ 07801
1	Commander US Army Aviation Research and Development Command ATTN: DRSVA-E 12th and Spruce Streets St. Louis, MO 63166	1	Commander US Army Harry Diamond Labs ATTN: DRXDO-TI 2800 Powder Mill Road Adelphi, MD 20783
1	Director US Army Air Mobility Research and Development Laboratory Ames Research Center Moffett Field, CA 94035	1	Director US Army TRADOC Systems Analysis Agency ATTN: ATAA-SL (Tech Lib) White Sands Missile Range NM 88002
1	Commander US Army Electronics Command ATTN: DRSEL-RD Fort Monmouth, NJ 07703	1	Texas Tech University Department of Chemistry ATTN: Dr. T. A. Caughey Lubbock, TX 79410
1	Commander US Army Missile Research and Development Command ATTN: DRDMI-R Redstone Arsenal, AL 35809		<u>Aberdeen Proving Ground</u> Marine Corps LnO Dir, USAMSAA
1	Commander US Army Tank-Automotive Development Command ATTN: DRDTA-RWL Warren, MI 48090		